CrystEngComm

ROYAL SOCIETY OF CHEMISTRY

PAPER

Cite this: *CrystEngComm*, 2020, **22**, 6128

Solid-state properties, solubility, stability and dissolution behaviour of co-amorphous solid dispersions of baicalin†

Ashok Kumar Jangid,[a] Poonam Jain,[a] Kanakaraju Medicherla,[b] Deep Pooja*[c] and Hitesh Kulhari *[a]

Received 22nd May 2020,
Accepted 14th August 2020

DOI: 10.1039/d0ce00750a

rsc.li/crystengcomm

Baicalin (BL) is a natural, potential therapeutic molecule with a wide range of biological activities. However, poor aqueous solubility, low stability, and slow dissolution are the major limitations of BL. Co-amorphous systems are new and emerging systems that are single-phase, multicomponent amorphous systems consisting of one or more small co-former with a hydrophobic drug. The co-former helps in improving the physicochemical properties of the hydrophobic drug without affecting its pharmacological properties. The objective of this study was to prepare co-amorphous solid dispersions of baicalin (BSDs) using organic acids and amino acids to enhance its solubility, stability and dissolution profiles. The BSDs were prepared in a molar ratio of 1 : 1 of drug and co-former by the solvent evaporation method. The prepared BSDs were characterized by powder XRD and DSC analysis for determining the physical solid-state of BL, and by FTIR to determine possible intermolecular interactions between BL and co-formers. The BSD prepared with histidine (BL–His) showed a perfect co-amorphous system with an approximately 60-fold increase in solubility, complete loss of crystallinity, and complete dissolution of BL within 15 min in simulated intestinal buffer. Further, BL–His showed physicochemical stability over a period of six months without any sign of recrystallization and loss of drug. Therefore, instead of the native and crystalline BL, the use of BL–His could be a better approach for pharmaceutical applications of BL.

1. Introduction

The discovery and development of a new drug molecule is a time consuming and costly process. This process is further hammered by the poor physicochemical properties of the developed new chemical entity (NCE). The poor physicochemical properties are mostly led by the low water solubility of the NCE. As per an estimate, about 40% of new oral drugs and about 70% of NCEs in the pharmaceutical industry pipelines are practically insoluble (*i.e.*, <0.1 mg mL^{-1}) in water. This aqueous insolubility of molecules is responsible for their slow dissolution and low oral bioavailability.[1,2] Poorly water-soluble drugs dissolve slowly in biological fluids and reach the systemic circulation at very low concentrations.[3,4] The poor solubility and low bioavailability result in therapeutic failure, high-fallout rate and increase in manufacturing costs.[5,6] To achieve a therapeutic concentration, these new oral drugs need to be administered at a high dose which leads to severe side effects and increases the cost of the formulations.[7]

The crystalline physical state of NCEs is one of the main reasons for their low aqueous solubility. The crystalline state is a thermodynamically stable, low energy state but is generally less soluble in water than the amorphous state. In contrast, the amorphous state shows high aqueous solubility but is thermodynamically less stable due to high energy. Therefore, the formulations developed with amorphous drugs fail clinically due to recrystallization of drugs during the processing and storage.[8]

To address the problems of poor aqueous solubility and slow dissolution of therapeutic molecules due to their crystalline state, various strategies like inclusion complexes, solid dispersions, micro-emulsions, *etc.* are being used.[9–12] The drug-excipient-based co-amorphous solid dispersion strategy has recently been getting more attraction than other techniques.[13,14] It is a highly effective, simple, and low-cost technique to improve the solubility and dissolution of poorly water-soluble, crystalline drugs.[15] Although the direct conversion of a crystalline drug molecule into an amorphous drug improves its solubility, the recrystallization of the drug over time remains an issue. So,

[a] *School of Nano Sciences, Central University of Gujarat, Gandhinagar-382030, Gujarat, India. E-mail: hitesh.kulhari@cug.ac.in*
[b] *Department of Human Genetics, College of Science and Technology, Andhra University, Visakhapatnam-530003, Andhra Pradesh, India*
[c] *The Centre for Advanced Materials & Industrial Chemistry (CAMIC), School of Science, RMIT University, Melbourne-3000, Australia. E-mail: d.dpooja00@gmail.com*
† Electronic supplementary information (ESI) available. See DOI: 10.1039/d0ce00750a

during amorphization, a stabilizing agent, called co-former, is used to prevent crystal growth.[16] Thus, a co-amorphous formulation contains the drug molecule in an amorphous state which is maintained by one or more co-formers.

Generally, co-amorphous solid dispersions are prepared using a polymer or a small molecule like sugar, organic acid, amino acid, *etc.* Small molecule-based co-amorphous systems (SMCS) are preferred over polymer-based co-amorphous systems due to their several advantages. Polymer-based co-amorphous systems have the disadvantages of limited miscibility of drug with polymers, phase separation and hygroscopic nature of polymers. On the other hand, SMCS have the advantages of higher intermolecular interactions, conformational flexibility and molecular level mixing which prevent phase separation and recrystallization.[17] In the past few years, several small molecules like amino acids, sugars, organic acids, *etc.* have been attempted as co-formers to develop co-amorphous formulations. A tremendous increase in the solubility and stability of hydrophobic drugs have been observed with their co-amorphous formulations. For instance, arginine as a co-forming agent increased the solubility of indomethacin 200 times in comparison to crystalline indomethacin.[18]

Baicalin (BL, 5,6-dihydroxyflavone-7-*O*-D-glucuronic) is the main bioactive flavone found in *Scutellaria baicalensis* and widely used in China, Japan and Korea as herbal medicine for the treatment of fever, inflammation and allergic diseases. BL also possesses numerous pharmacological and therapeutic activities such as antioxidant, antiviral, antiarthritic, antifertility, antiplasmodic, antitumor, and anti-inflammatory activities.[19–22] However, the potential therapeutic benefits of BL at preclinical and clinical stages are limited due to its poor aqueous solubility and low oral bioavailability (2.2%) in rats.[23] Further, it interacts with co-administered drugs and induces the activity of metabolizing enzyme cytochrome P450. After the oral administration of BL, five types of secondary metabolites have been identified and these metabolites are rapidly hydrolysed by β-glucuronidase/sulfatase enzymes.[24]

In the past few years, several BL formulations like solid-lipid nanoparticles,[25] nanocrystals,[26] micelles,[27] liposomes[28] and nanoemulsions[29] have been developed to improve the solubility and oral bioavailability of BL. However, these formulations still have challenges of scale-up, long term stability and rapid recrystallization. Therefore, in this study we have designed a scalable co-amorphous solid dispersion formulation of BL to enhance its solubility, stability and dissolution.

2. Materials and methods

2.1 Materials

Baicalin (BL) was obtained from TCI Chemicals (USA). Citric acid (CA), fumaric acid (FA), oxalic acid (OA), glutamic acid (Glu), asparagine (Asp), histidine (His) and methanol were purchased from Loba Chemie (Mumbai, India). All other chemicals and solvents were purchased from Rankem (Mumbai, India).

2.2 Preparation of baicalin solid dispersions (BSDs)

The BL solid dispersions (BSDs) were prepared by the solvent evaporation method. Crystalline BL and different co-formers (organic acids or amino acids) were mixed in a 1 : 1 molar ratio using a mortar and pestle for 2 min and then transferred in a round bottom flask (RBF) containing 15 mL of methanol. The resulting mixture was stirred magnetically for 6 h at room temperature. After that, methanol was evaporated using a rotary evaporator and a thin layer was obtained in the RBF. The resulting thin layer of the mixture was dissolved in 10 mL of Milli-Q water and sonicated for 5 min at a frequency of 25 Hz. Thereafter, the mixture was lyophilized and was used for further analysis. The physical mixtures (premix) of pure BL and co-formers (in a 1 : 1 molar ratio) were prepared by direct mixing using a mortar and pestle for 2 min.

2.3 Powder X-ray diffraction analysis

The PXRD patterns of BL and BSDs were obtained using an X-ray diffractometer (D8 Advance, Bruker, Germany) equipped with a Cu-Kα X-ray radiation source. The instrument was set at 40 kV and 30 mA and the diffraction patterns were measured from 5° to 80°. The percentage crystallinity (%*C*) of BSDs was estimated using the following equation.[30]

$$\%C = \left[\frac{A1_{\text{crystalline peaks}} \times 100}{A2_{\text{crystalline and amorphous phases}}}\right]$$

$A1$ = area contribution from crystalline peaks; $A2$ = area contribution from the crystalline and amorphous phases.

2.4 Differential scanning calorimetry

The DSC analysis of BL and prepared BSDs was performed on a DSC 4000 Perkin Elmer instrument under a nitrogen flow of 20 mL min^{-1}. The samples (about 3.5 mg) were sealed in aluminium pans and heated at a heating rate of 10 °C min^{-1}.

2.5 Fourier transform infrared spectroscopy

The FTIR spectra of BL and BSDs were obtained using an FTIR spectrophotometer (Perkin Elmer spectrum). For this, the samples were mixed with anhydrous KBr, pelletized using a hydraulic press and scanned for % transmittance in the range of 4000 to 400 cm^{-1}.

2.6 Drug content determination studies

The BL content was determined by dissolving 10 mg of lyophilized BSDs in methanol. The solutions were then vortexed for 2 min and filtered using a membrane filter of pore size 0.22 μm. After appropriate dilution, the BL content was determined using a UV-visible spectrophotometer at 277 nm.

2.7 Solubility studies

The solubility of BL and different BSDs in water and different buffer media, *i.e.* 0.1 N HCl (pH 1.2), sodium acetate buffer (SAB, pH 5.0), phosphate buffered saline (PBS, pH 7.4) and 0.1 N Tris base buffer (TB, pH 9.0), was determined by the shake flask method. An excess of BL or BSD powder (250 mg) was added into amber-coloured glass vials containing 5 mL of Milli-Q water or buffer solutions. The samples were placed in an orbital shaker (Thermo Scientific, SHKE6000-8CE) maintained at 37 °C for 12 h. These samples were centrifuged at 6000 rpm for 10 min, filtered through 0.22 μm membrane syringe filters and analysed for BL content using a UV-vis spectrophotometer at 277 nm.

2.8 *In vitro* dissolution studies

The dissolution study was performed in dissolution tester apparatus (DS 8000, LABINDIA). The pellets of crystalline BL or BSDs (equivalent to 100 mg BL) were prepared by directly compressing into a hydraulic press machine at 124.9 MPa for 60 s. The pellets were placed in 900 mL of 0.1 N HCl (pH 1.2) or 0.01 M phosphate buffer (pH 6.8) as the dissolution medium at a temperature of 37 ± 0.5 °C and stirred with a paddle set at 100 rpm. At pre-set time points (0, 5, 10, 15, 20, 25, 30, 45, 60, 90 and 120 min), 2 mL aliquots were withdrawn and replaced with an equal volume of fresh dissolution medium. The samples of each time point were filtered through a 0.22 μm membrane syringe filter and analysed for %BL content using a UV-vis spectrophotometer at 277 nm.

2.9 Physical stability of BSDs

The BSDs were stored in a desiccator under dry conditions at room temperature for 6 months. After that, the samples were analysed by powder XRD to investigate the possible recrystallization of BL and co-formers.

2.10 Chemical stability of BSDs

The chemical stability of the BSDs was determined by measuring the %BL content after 6 months of storage. For this, 2 mg of BSDs was dissolved in an appropriate amount of water and determined for % drug content using a UV-vis spectrophotometer at 277 nm.

2.11 Data analysis

The experiments were performed in triplicate and the results are reported as mean ± standard deviation (n = 3).

3. Results and discussion

The development of a co-amorphous system of a lipophilic and crystalline molecule has the advantages of higher aqueous solubility and better dissolution in biological systems than the native molecule. The solid-state properties of native BL and BSDs were determined by PXRD, DSC and FTIR analysis.

3.1 Powder X-ray diffraction analysis

PXRD is the most convincing technique for determining the physical state of a molecule. The PXRD pattern of a crystalline molecule shows sharp intense peaks. In our study, the semi-crystalline state of BL was obtained in BSDs prepared with organic acids and two (glutamic and asparagine) amino acids (Fig. 1). However, the BSD with histidine (His) showed the complete amorphous form of BL. Fig. 2 shows the PXRD patterns of pure BL, co-formers, a physical mixture of BL and co-former (premix), and prepared BSDs. Pure BL showed characteristic peaks at 2θ angles of 8.5°, 10.3°, 12.2°, 14.4°, 16.8°, 20.5°, 23.6°, 25.2°, 27.8°, and 29.3°.[31] These sharp and highly intense peaks of BL clearly demonstrated the crystalline state of BL. On the other hand, the used co-formers showed the crystalline state with intense peaks in the 2θ range of 10–50°. The PXRD patterns of the premix displayed the peaks of both crystalline BL and used co-formers. The PXRD patterns of the prepared BSDs, except BL–His BSD, show few intense peaks with slight shifting. It shows the formation of co-crystals BSDs with CA, FA, OA, Glu and Asp. The intense peaks were observed at 8.3°, 20.4° and 25.1° with BL–CA BSDs, at 8.3°, 14.6° and 25.3° with BL–FA BSDs, and at 8.3°, 12.4°, 14.5°, 16.9°, 20.5°, 22.3°, 23.6°, 25.2° and 27.9° with BL–OA BSDs. Similarly, the amino acid BSD peaks were observed at 2θ angles of 8.3°, 10.3°, 12.4°, 14.4°, 20.5° and 27.9° with BL–Glu BSDs, and at 8.3°, 14.7°, 25.1°, 28.1° and 29.1° with BL–Asp BSDs. The

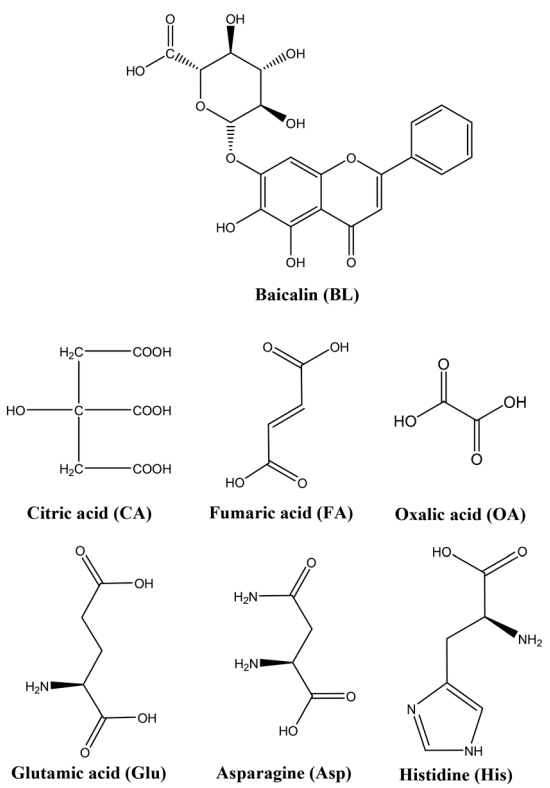

Fig. 1 Molecular structures of pure baicalin and other co-formers used in this study.

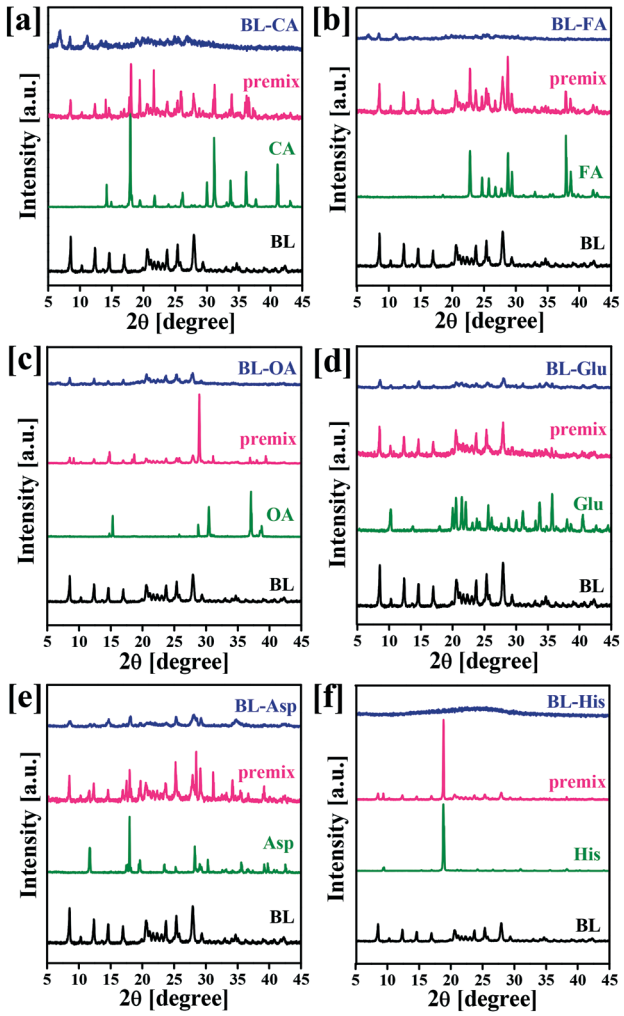

Fig. 2 Powder XRD patterns of baicalin solid dispersions: (a) BL–citric acid (BL–CA), (b) BL–fumaric acid (BL–FA), (c) BL–oxalic acid (BL–OA), (d) BL–glutamic acid (BL–Glu), (e) BL–asparagine (BL–Asp) and (f) BL–histidine (BL–His).

results suggested that these systems formed co-crystals instead of co-amorphous phases. Further, the observed PXRD peaks were different from the original state of pure BL and co-former agents. Interestingly, the BSD prepared with His (BL–His) did not show any peak in the 2θ range of 10–80°, rather a hump was observed in the 2θ range of 18–28°. This indicates that BL was completely converted into an amorphous phase with His.

To further evaluate the phase conversion of BL in different BSD formulations, the decrease in crystallinity of BL was determined. Table 1 shows the calculated % crystallinity (%C) of the prepared BSDs using the collected PXRD data (Fig. S1†). The total areas of crystalline and amorphous phases underneath the diffractograms were calculated using 2θ values from 5° to 30°.[30,32] In order to separate the contribution from crystalline and amorphous peaks, the ratio of the integrated area of crystalline peaks to the total integrated area from the crystalline and amorphous XRD peaks was obtained. The results indicated that the decrease

Table 1 Crystallinity (%C) of the prepared different baicalin solid dispersion (BSD) formulations

System	%C
BL–CA	27.67
BL–FA	16.97
BL–OA	71.85
BL–Glu	46.56
BL–Asp	38.27
BL–His	0.00

in the crystallinity was highest with BL–FA followed by BL–CA and BL–OA. The %C of co-crystals prepared with CA, FA and OA was observed to be 27.6, 16.9 and 71.8%, respectively. In the case of BSDs prepared with amino acids, BL–His showed a complete loss of crystallinity of BL during processing and preparation of the formulation and thus presented a perfect co-amorphous formation. BL–Glu and BL–Asp showed the formation of co-crystals with %C of BL of about 46.5% and 38.2%, respectively.

3.2 Differential scanning calorimetry analysis

The thermal behaviour of pure BL and prepared BSD systems was determined by DSC analysis which gives an insight into the melting point and recrystallization behaviour of solid and amorphous materials.[25] Fig. 3 shows the DSC scan of pure BL and prepared BSD formulations where the pure DSC scan of BL was compared with those of the formed BSDs. Based on the observed results, pure BL showed a sharp endothermic peak at 145 °C and 210 °C. The peak at 145 °C may be due to the dehydration of BL while the peak at 210 °C corresponds to its melting point.[31] The absence or shifting of these peaks of BL in the BSD formulations indicated the phase transformation of BL. The glass transition temperatures (T_g) of pure BL and prepared BSD formulations were determined and are shown in Fig. S2.† The observed T_g of BSDs showed a shift from the T_g of pure crystalline BL. BL showed a T_g at 101 ± 0.5 °C which was shifted in all the prepared BSDs to 97 ± 0.8 °C, 51 ± 0.9 °C, 55 ± 0.4 °C, 99 ±

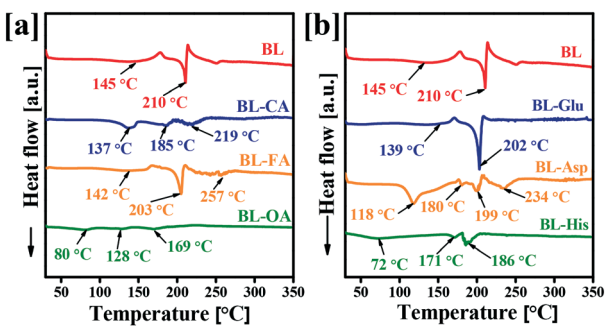

Fig. 3 Differential scanning calorimetry analysis of baicalin (BL) and different baicalin solid dispersions: (a) with citric acid (BL–CA), fumaric acid (BL–FA) and oxalic acid (BL–OA), and (b) with glutamic acid (BL–Glu), asparagine (BL–Asp) and histidine (BL–His).

0.9 °C, 52 ± 0.7 °C and 38 ± 0.6 °C with CA, FA, OA, Glu, Asp and His, respectively. Hence, compared to pure BL, the DSC scans of BSD formulations showed significant shifts and suggested the changes in the crystalline state of BL to another state like a polymorphous or amorphous state.[33–36]

3.3 Fourier transformation infrared spectroscopy analysis

FTIR analysis of solid dispersions provides important information about the change in the molecular arrangement of components of the system.[37] It also helps in determining the possible interactions like hydrogen bonding and π–π interaction between the drug and co-forming agent.[38] As BL and the used co-formers have functional groups like hydroxyl, carboxylic and amine groups, there are more chances of interaction *via* hydrogen bonding.[39,40] BL has five hydroxyl groups and one carboxylic group while organic acids have carboxylic groups, and amino acids have both amine and carboxylic groups available for possible interactions.[41] Fig. S3† shows the FTIR spectra of pure BL, co-formers, premix and BSDs where the –OH and >C=O peaks were mainly observed (Fig. 4 and 5). Pure crystalline BL showed characteristic peaks at 3557 and 3493 cm^{-1} for –OH stretching, 1726 cm^{-1} and 1660 cm^{-1} for carbonyl (>C=O), 1609, 1572 and 1495 cm^{-1} for C=C of phenyl, and 1064 cm^{-1} for C–O–C in the ether and hydroxyl groups.

There was no change in the peaks of BL in the FTIR spectra of premixes. However, the FTIR spectra of BSDs showed a significant shift in characteristic peaks of BL which may be due to the interaction between BL and co-formers through hydrogen bonding (Table S1†). A significant shift in the >C=O stretching frequencies was observed in BSDs. Fig. 4 shows a closer look in the >C=O region of the FTIR spectra. The peaks were shifted and found to be broader as compared to those of pure BL. The peaks for >C=O frequencies were observed at 1731 cm^{-1} with CA, at 1758 and 1729 cm^{-1} with FA, at 1729 cm^{-1} with OA, at 1728 and 1659 cm^{-1} with Glu, at 1727 and 1659 cm^{-1} with Asp and at 1667

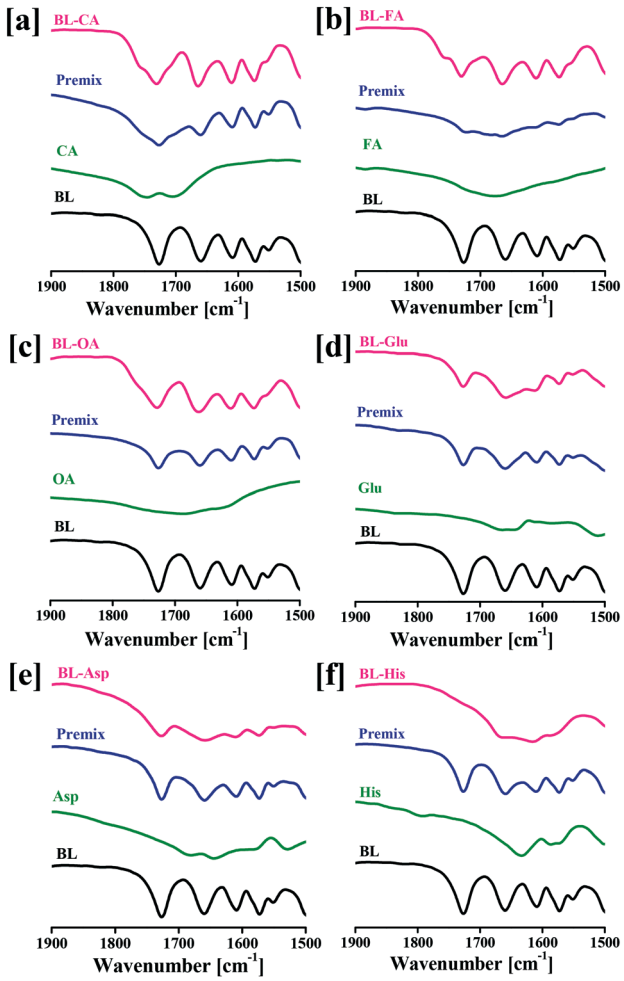

Fig. 4 FTIR spectra of the >C=O stretching region in the baicalin solid dispersions (BSDs) prepared with different co-formers: (a) BL–citric acid (BL–CA), (b) BL–fumaric acid (BL–FA), (c) BL–oxalic acid (BL–OA), (d) BL–glutamic acid (BL–Glu), (e) BL–asparagine (BL–Asp) and (f) BL–histidine (BL–His).

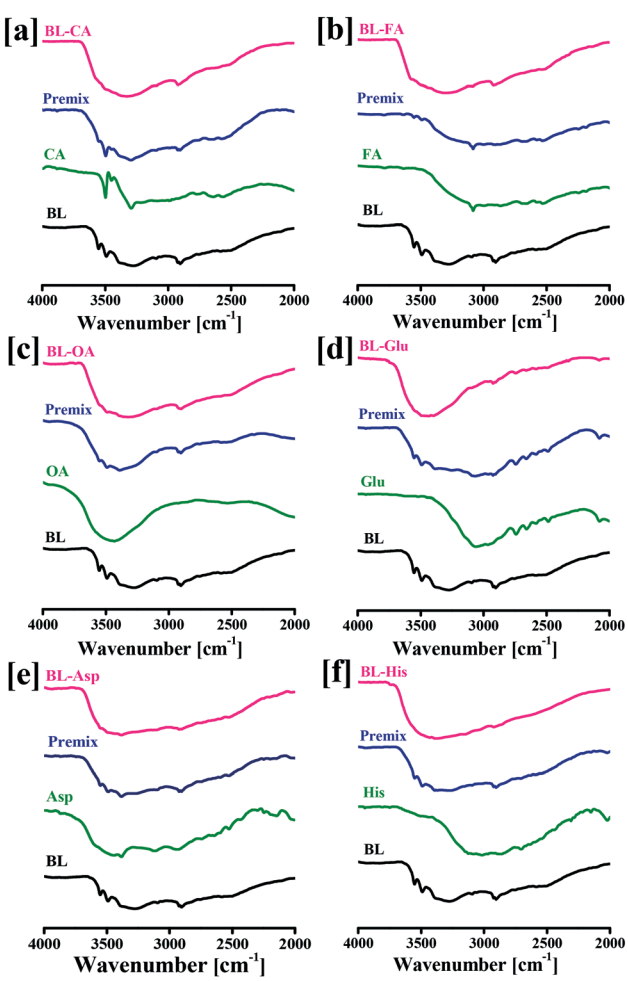

Fig. 5 FTIR spectra of the –OH stretching region in the baicalin solid dispersions (BSDs) prepared with different co-formers: (a) BL–citric acid (BL–CA), (b) BL–fumaric acid (BL–FA), (c) BL–oxalic acid (BL–OA), (d) BL–glutamic acid (BL–Glu), (e) BL–asparagine (BL–Asp) and (f) BL–histidine (BL–His).

and 1614 cm^{-1} with His (Fig. 4). These significant changes in peak positions suggested the involvement of the >C═O moiety of co-formers in their interaction with BL. Further, a significant difference in the –OH stretching in BSD formulations was observed in comparison to pure BL. The –OH stretching peak of BL was transformed into shoulder peaks along with a shift in the peak position (Fig. 5). Thus, these shifted peaks confirmed the formation of hydrogen bonding between BL and co-formers, resulting in the formation of BSDs.[41–43]

3.4 Determination of BL content in BSDs

The amount of BL present in various BSD formulations was determined and is presented in Fig. 6. About 428.3 ± 8.9, 582.7 ± 6.7, 648.4 ± 9.1, 447.8 ± 8.8, 640.9 ± 9.8 and 542.2 ± 6.3 μg of BL was found to be present in per mg of BL–CA, BL–FA, BL–OA, BL–Glu, BL–Asp, and BL–His, respectively.

3.5 Effect of the formation of BSDs on the solubility of BL

The solubility of BL in water was found to be 0.043 mg mL^{-1} at room temperature. In co-crystal BSDs, prepared with organic acids, the solubility of BL was 0.269, 0.141 and 0.295 mg mL^{-1} with CA, FA and OA, respectively (Fig. 7). The aqueous solubility of BL was enhanced significantly, 6.2 times with CA, 3.4 times with OA and 6.8 times with FA co-crystals in water. This can be explained by the molecular interactions like hydrogen bonding with the carboxylic group of organic acids and the hydroxyl group of carboxylic groups of BL. The highest solubility of BL was observed with FA which could be attributed to the presence of free functional groups (two carboxylic groups and one hydroxyl group) for hydrogen bonding.[44]

In the case of BSDs prepared with amino acids, the highest solubility of BL was observed with His (2.652 mg mL^{-1}) followed by Asp (0.284 mg mL^{-1}) and Glu (0.112 mg mL^{-1}) in water. The water solubility enhanced by Asp and Glu is comparable to that observed with organic acids and can be explained by the hydrogen bonding between amino acids and BL molecules. However, the BSD prepared with His showed a 60-fold increase in the aqueous solubility of BL. The reason

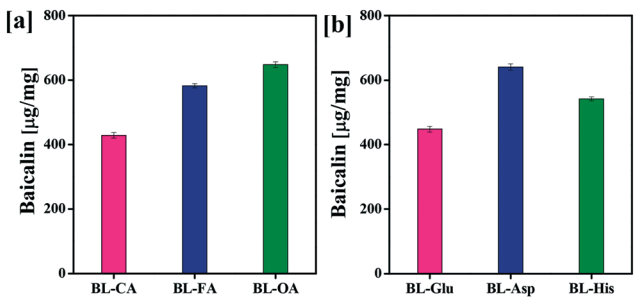

Fig. 6 Quantitative analysis of different baicalin solid dispersions (BSDs): (a) baicalin–citric acid (BL–CA), baicalin–fumaric acid (BL–FA), and baicalin–oxalic acid (BL–OA); (b) baicalin–glutamic acid (BL–Glu), baicalin–asparagine (BL–Asp), and baicalin–histidine (BL–His).

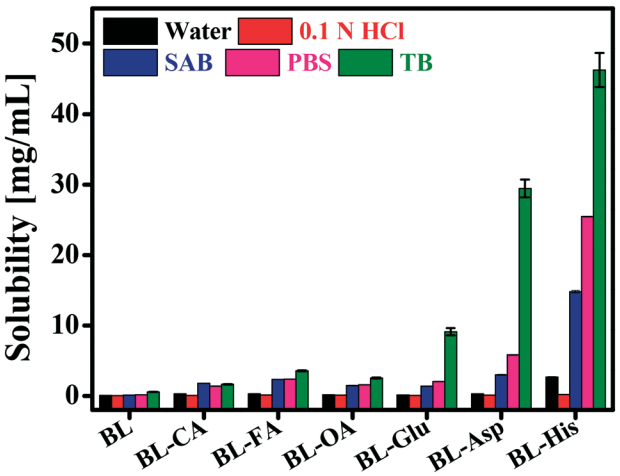

Fig. 7 Solubility (mg mL^{-1}) of baicalin (BL) and different BL solid dispersions (BSDs) in different media (SAB: sodium acetate buffer (pH 5.0), PBS: phosphate buffered saline (pH 7.4) and TB: Tris base buffer (pH 9.0)).

for this remarkable increase in solubility of BL is the formation of ionisable zwitterionic SDs and BL–His salt.[37,45] Further, His contains an electron-rich aromatic (imidazole) ring in addition to the other sites for hydrogen bonding. Therefore, it could interact with BL through both hydrogen bonding and π–π interactions. The higher aqueous solubility of BL–His could also be attributed to the complete conversion of crystalline BL into amorphous BL.

The %crystallinity of the co-crystals prepared with different organic acid co-formers was found to be BL–OA (71.8%) > BL–CA (27.6%) > BL–FA (16.9%). With amino acid co-formers, the observed %crystallinity was in the order of BL–Glu (46.5%) > BL–Asp (38.2%) > BL–His (0%) (Table 1). The solubility of BSD formulations in water was observed in the following order: BL–FA > BL–CA > BL–OA (with organic acids) and BL–His > BL–Asp > BL–Glu (with amino acids). From the observed results, it has been concluded that the solubility of BSD formulations in water increased with decreasing %*C* value.

The solubility of the prepared BSDs was also determined in different pH media, *i.e.* 0.1 N HCl (pH 1.2), SAB, PBS, and TB. Pure BL showed a pH-dependent change in its solubility. The solubility of BL was increased with an increase in the pH of media. The observed solubility of BL was 0.025, 0.08, 0.14 and 0.56 at pH 1.2, pH 5.0, pH 7.4 and pH 9.0, respectively. The higher solubility of BL at basic pH could be attributed to its ionization.[46] The carboxylic acid group of BL is ionized or deprotonated at basic pH and responsible for the increase in solubility of BL. A similar trend was observed with the different BSD formulations. BL–His showed an approximately 82-fold increase in the solubility of BL in TB. Importantly, the solubility of BL–His was increased 180 times in PBS which represents the blood pH and is the one of the most commonly used solvents for pharmaceutical formulations. These data clearly show the advantage of the designed formulation of BL over the native BL.

3.6 Dissolution study

The dissolution profiles of native BL and the prepared BSDs systems were determined in 0.1 N HCl (pH 1.2) and phosphate buffer (pH 6.8) and are shown in Fig. 8. As compared to pure BL, BSDs exhibited faster dissolution behaviour in both pH 1.2 and pH 6.8 buffer solutions. BL–His and BL–OA showed higher dissolution than the other corresponding BSDs. In 0.1 N HCl (pH 1.2) medium, the %BL dissolved was in the order of BL–His (28.8%) > BL–Asp (9.3%) > BL–Glu (6.4%) (with amino acids) and BL–FA (15.4%) > BL–OA (6.5%) > BL–CA (6.4%) (with organic acids) after 2 h. Thus, the higher dissolution of BL–His and BL–OA BSDs in 0.1 N HCl buffer solution could be attributed to the decrease in crystallinity and higher solubility than the other BSDs. In PB (pH 6.8), pure BL was dissolved by about 63.4% in the first 30 min while the solid dispersion formulations showed complete dissolution in the same time. About 96.1, 92 and 98.4% of BL was dissolved from organic acid-based BSDs, *i.e.* BL–OA, BL–CA, and BL–FA, respectively. Similarly, with amino acid BSD systems, about 97.7, 90.3 and 98.5% of BL was dissolved from BL–Asp, BL–Glu, and BL–His, respectively. These results revealed the pH-dependent dissolution of BL in BSDs and it could be directly correlated with the pH-dependent solubility of BL. The solubility of BL increases with an increase in the pH of the media due to its ionization at basic pH.[47] Further, the difference in the dissolution behaviour of the different BSDs can also be explained by the difference in different crystalline contents of BL in BSDs.[22] As the crystallinity of BSDs decreased (Table 1), both the solubility and dissolution of BSD formulations were increased.

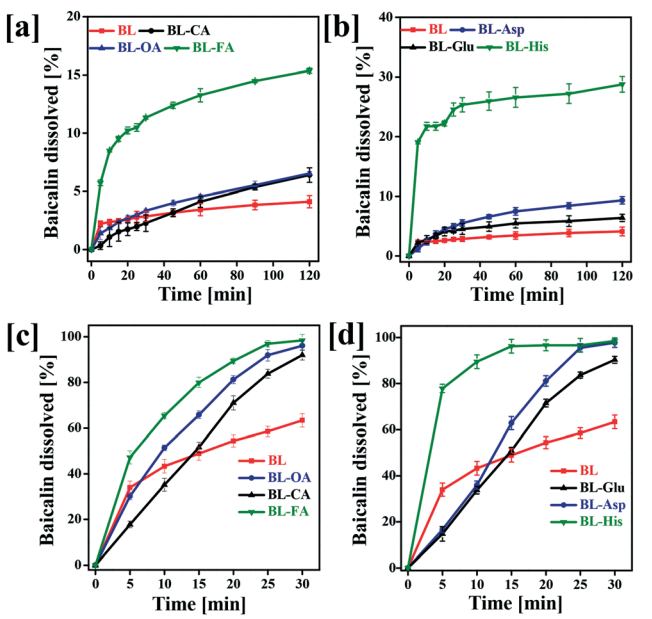

Fig. 8 Dissolution profiles of crystalline BL and baicalin solid dispersions: (a) BL–organic acids in 0.1 N HCl at pH 1.2, (b) BL–amino acids at pH 1.2, (c) BL–organic acid at pH 6.8, and (d) BL–amino acids in phosphate buffer at pH 6.8 (mean ± standard deviation, n = 3).

3.7 Physical stability

The effect of storage conditions on the physical stability of BL in different BSD formulations was ensured by PXRD studies. The physical stability of BSDs was evaluated in terms of the observed re-crystallization before and after 6 months of storage. As shown in Fig. 9, the crystallinity of BL was observed in BSDs prepared with CA, FA, OA, Glu and Asp. The PXRD patterns of BL–CA, BL–FA, BL–OA, BL–Glu and BL–Asp BSDs show a slightly increase in crystallinity (Fig. 9a–e) and sharp peaks, observed after 6 months of storage. The BL–His formulation, which was completely converted into an amorphous phase, did not show any sign of recrystallization of BL (Fig. 9f). Compared to all the BSDs, BL–His showed the highest physical stability which could be attributed to the strong hydrogen bonding and π–π interactions between BL and His. It has also been reported previously that the stability of a drug molecule in solid dispersions depends on its ability to electrostatically interact with the co-former.[13,48]

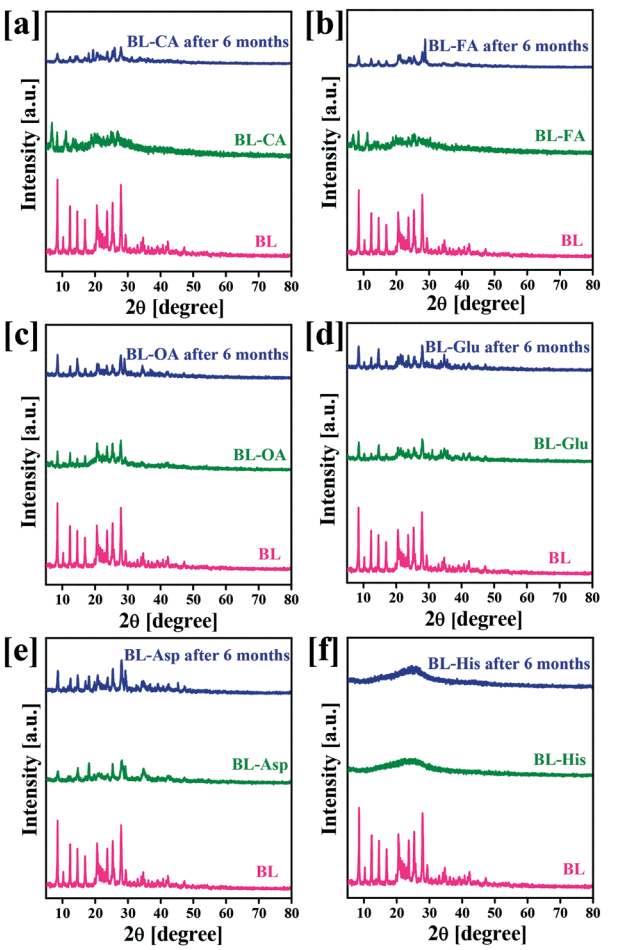

Fig. 9 Powder X-ray diffraction patterns of baicalin (BL) and BL solid dispersions (BSDs) after 6 months of storage at room temperature. BSDs were prepared with (a) citric acid (BL–CA), (b) fumaric acid (BL–FA), (c) oxalic acid (BL–OA), (d) glutamic acid (BL–Glu), (e) asparagine (BL–Asp) and (f) histidine (BL–His).

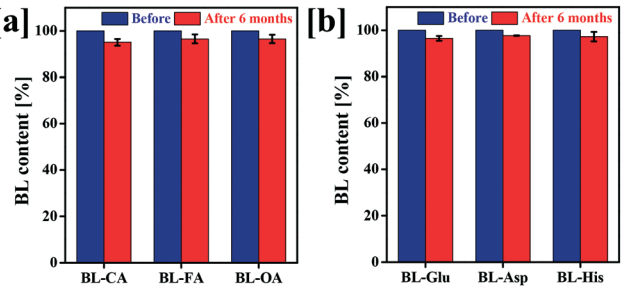

Fig. 10 Chemical stability of baicalin solid dispersions prepared with (a) organic acids and (b) amino acids.

3.8 Chemical stability

Fig. 10 shows the chemical stability of BL in different BSDs. More than 95% of BL content was found in all the BSDs after six months of storage. This suggested that the BSD formulations were stable for a long time and BL was chemically stable in the matrices of the formulations.

4. Conclusion

In the present study, different organic and amino acids were used as co-formers to prepare solid dispersions to enhance the aqueous solubility, dissolution, and stability of BL. These changes in the physicochemical properties of BL, after its conversion into a co-amorphous system, could be attributed to the non-covalent interactions between BL and co-formers. Among the prepared formulations, the highest solubility and the fastest dissolution rate were observed with His which could be explained by the complete amorphization of BL with His as observed by PXRD analysis. Importantly, the results of the stability studies clearly revealed the stabilization of BL in an amorphous phase over a period of six months. Therefore, the developed BL–His system could be used in designing pharmaceutical dosage forms of BL with improved aqueous solubility, dissolution and physicochemical stability.

Conflicts of interest

The authors declare no conflict of interest.

Acknowledgements

The authors would like to thank the Central University of Gujarat, Gandhinagar for providing necessary facilities and support. HK acknowledges the Department of Science and Technology, New Delhi for an INSPIRE Faculty Award. AKJ and PJ acknowledge the University Grant Commission, New Delhi for a PhD. fellowship.

References

1 A. Singh and G. Van den Mooter, *Adv. Drug Delivery Rev.*, 2016, **100**, 27–50.
2 R. Censi and P. Di Martino, *Molecules*, 2015, **20**, 18759–18776.
3 J. Li, Y. Yang, L. Lu, Q. Ma and J. Zhang, *Int. J. Nanomed.*, 2018, **13**, 2129–2141.
4 H. Ueda, W. Wu, K. Lo, H. Grohganz and A. Mu, *Mol. Pharmaceutics*, 2018, **15**, 2036–2044.
5 D. Pooja, H. Kulhari, M. Kuncha, S. S. Rachamalla, D. J. Adams, V. Bansal and R. Sistla, *Mol. Pharmaceutics*, 2016, **13**, 3903–3912.
6 D. Pooja, H. Kulhari, M. K. Singh, S. Mukherjee, S. S. Rachamalla and R. Sistla, *Colloids Surf., B*, 2014, **121**, 461–468.
7 C. Mocktar and T. Govender, *Mol. Pharmaceutics*, 2018, **15**, 3512–3526.
8 A. Karagianni, K. Kachrimanis and I. Nikolakakis, *Pharmaceutics*, 2018, **10**(3), 98–124.
9 S.-H. Ren, J.-Q. Zhang, H.-H. Yan, X. Zheng, H.-Y. Zhu, Y. Jin and J. Lin, *J. Inclusion Phenom. Macrocyclic Chem.*, 2016, **85**, 317–328.
10 A. A. Muthu Prabhu, G. Venkatesh and N. Rajendiran, *J. Solution Chem.*, 2010, **39**, 1061–1086.
11 D. Sharma and S. Joshi, *Asian J. Pharm.*, 2007, **1**, 1–11.
12 R. M. Shah, D. S. Eldridge, E. A. Palombo and I. H. Harding, *Eur. J. Pharm. Biopharm.*, 2017, **117**, 141–150.
13 M. H. Fung, M. Devault, K. T. Kuwata and R. Suryanarayanan, *Mol. Pharmaceutics*, 2018, **15**(3), 1052–1061.
14 P. Tran, Y.-C. Pyo, D.-H. Kim, S.-E. Lee, J.-K. Kim and J.-S. Park, *Pharmaceutics*, 2019, **11**, 132.
15 Y. Wang, C. Wang, J. Zhao, Y. Ding and L. Li, *J. Colloid Interface Sci.*, 2017, **485**, 91–98.
16 J. M. Skieneh, I. Sathisaran, S. V. Dalvi and S. Rohani, *Cryst. Growth Des.*, 2017, **17**(12), 6273–6280.
17 R. B. Chavan, R. Thipparaboina, D. Kumar and N. R. Shastri, *Int. J. Pharm.*, 2016, **515**, 403–415.
18 Z.-L. Li, S.-F. Peng, X. Chen, Y.-Q. Zhu, L.-Q. Zou, W. Liu and C.-M. Liu, *Food Res. Int.*, 2018, **108**, 246–253.
19 Z. Feng, J. Zhou, X. Shang, G. Kuang, J. Han, L. Lu and L. Zhang, *Pharm. Biol.*, 2017, **55**, 1177–1184.
20 M. Haider, M. A. Hassan, I. S. Ahmed and R. Shamma, *Mol. Pharmaceutics*, 2018, **15**(8), 3478–3488.
21 X. Liu, Y. Chen, T. Qiu, Y. Chen and L. Wang, *J. Chem. Eng. Data*, 2009, **54**, 2330–2331.
22 J. Wan and W. Zhu, *Int. J. Nanomed.*, 2013, **8**, 2961–2973.
23 L. Zhao, W. Yumeng, Y. Huang, B. He, Y. Zhou and J. Fu, *Int. J. Nanomed.*, 2013, **8**, 3769–3779.
24 J. Xing, X. Chen and D. Zhong, *Life Sci.*, 2005, **78**, 140–146.
25 J. Hao, F. Wang, X. Wang, D. Zhang, Y. Bi, Y. Gao, X. Zhao and Q. Zhang, *Eur. J. Pharm. Sci.*, 2012, **47**, 497–505.
26 P.-F. Yue, Y. Li, J. Wan, Y. Wang, M. Yang, W.-F. Zhu, C.-H. Wang and H.-L. Yuan, *Int. J. Nanomed.*, 2013, **8**, 2961–2973.
27 H. Zhang, X. Yang, L. Zhao, Y. Jiao, J. Liu and G. Zhai, *Drug Delivery*, 2016, **23**, 1933–1939.
28 Y. Wei, J. Guo, X. Zheng, J. Wu, Y. Zhou, Y. Yu, Y. Ye, L. Zhang and L. Zhao, *Int. J. Nanomed.*, 2014, **9**, 3623–3630.
29 L. Wu, Y. Bi and H. Wu, *Drug Dev. Ind. Pharm.*, 2018, **44**, 266–275.
30 A. S. Zidan, Z. Rahman, V. Sayeed, A. Raw, L. Yu and M. A. Khan, *Int. J. Pharm.*, 2012, **423**, 341–350.

31 Y. Li, Z. D. He, Q. E. Zheng, C. Hu and W. F. Lai, *Molecules*, 2018, **23**(5), 1169–1183.

32 S. Soisuwan, V. Teeranachaideekul, A. Wongrakpanich, P. Langguth and V. B. Junyaprasert, *Eur. J. Pharm. Biopharm.*, 2019, **137**, 68–76.

33 A. Alqurshi, K. L. A. Chan and P. G. Royall, *Sci. Rep.*, 2017, **7**, 1–16.

34 A. J. Smith, P. Kavuru, L. Wojtas, M. J. Zaworotko and R. D. Shytle, *Mol. Pharmaceutics*, 2011, 1867–1876.

35 N. P. Aditya, I. E. Hamilton, J. Noon and I. T. Norton, *ACS Sustainable Chem. Eng.*, 2019, **7**, 9771–9781.

36 A. Karagianni, K. Kachrimanis and I. Nikolakakis, *Pharmaceutics*, 2018, **10**, 98–124.

37 Y. Huang, Q. Zhang, J. R. Wang, K. L. Lin and X. Mei, *Pharm. Dev. Technol.*, 2017, **22**, 69–76.

38 G. Kasten, H. Grohganz, T. Rades and K. Löbmann, *Eur. J. Pharm. Sci.*, 2016, **95**, 28–35.

39 V. Sharma and K. Pathak, *Acta Pharm. Sin. B*, 2016, **6**, 600–613.

40 J. Fan, Y. Dai, H. Shen, J. Ju and Z. Zhao, *Molecules*, 2017, **22**(5), 776–787.

41 Y. Ishizuka, K. Ueda, H. Okada, J. Takeda, M. Karashima, K. Yazawa, K. Higashi, K. Kawakami, Y. Ikeda and K. Moribe, *Mol. Pharmaceutics*, 2019, **16**, 2785–2794.

42 G. Kasten, H. Grohganz, T. Rades and K. Löbmann, *Eur. J. Pharm. Sci.*, 2016, **95**, 28–35.

43 G. Kasten, L. Lobo, S. Dengale, H. Grohganz, T. Rades and K. Löbmann, *Eur. J. Pharm. Biopharm.*, 2018, **132**, 192–199.

44 J. Mishra, K. Löbmann, H. Grohganz and T. Rades, *Int. J. Pharm.*, 2018, **552**, 407–413.

45 K. Löbmann, H. Grohganz, R. Laitinen, C. Strachan and T. Rades, *Eur. J. Pharm. Biopharm.*, 2013, **85**, 873–881.

46 S. J. Bethune, N. Huang, A. Jayasankar and N. Rodríguez-Hornedo, *Cryst. Growth Des.*, 2009, **9**, 3976–3988.

47 L.-Y. Wang, Y.-M. Yu, F.-B. Jiang, Y.-T. Li, Z.-Y. Wu and C.-W. Yan, *New J. Chem.*, 2020, **44**, 3930–3939.

48 M. Fung, K. Berzins and R. Suryanarayanan, *Mol. Pharmaceutics*, 2018, **15**, 1862–1869.

